The characteristics and impacts of extreme Atlantic windstorms on Arctic warming

Ja-Young Hong, Baek-Min Kim, Eun-Hyuk Baek, and Joo-Hong Kim
Unit of Arctic Sea-Ice Prediction, Korea Polar Research Institute, Incheon, South Korea

Korea Polar Research Institute

1. Introduction

- The Arctic warming is most pronounced during fall and winter results from a combination of significant factors, including increased greenhouse gases and positive feedbacks concerning snow and sea ice, aerosol and black carbon, cloud cover and water vapor, surface thermal inversion, and atmospheric lapse-rate.
- In addition to these local sources, Arctic warming is linked to planetary-scale waves, stationary waves, and transient eddies which lead to an enhanced poleward energy transport by moisture intrusion from mid-latitude to the Arctic. However, the primary contributing factor of Arctic warming still remains a debated issue.
- The Arctic warming has an optimal circulation wave pattern to develop. It is the combination of the positive NAO pattern and atmospheric blocking over the Ural Mountains of western Russia. This stationary wave pattern of the Arctic warming is basically link to warmer sea surface temperature over the western North Atlantic Ocean which modulate the transient eddies.
- However, previous studies on Arctic warming have not focused on how much do strong windstorms statistically warms the Arctic temperature. Since most strong windstorms occur over the North Atlantic sector, here we classify the North Atlantic windstorms according to the storm intensities (minimum central pressures) during winter for the last 36 years (December-January-February 1981/82–2016/17), and explore their relationship to Arctic temperature and atmospheric circulation changes, particularly the Atlantic side of the Arctic Ocean.

2. Atlantic windstorm tracks

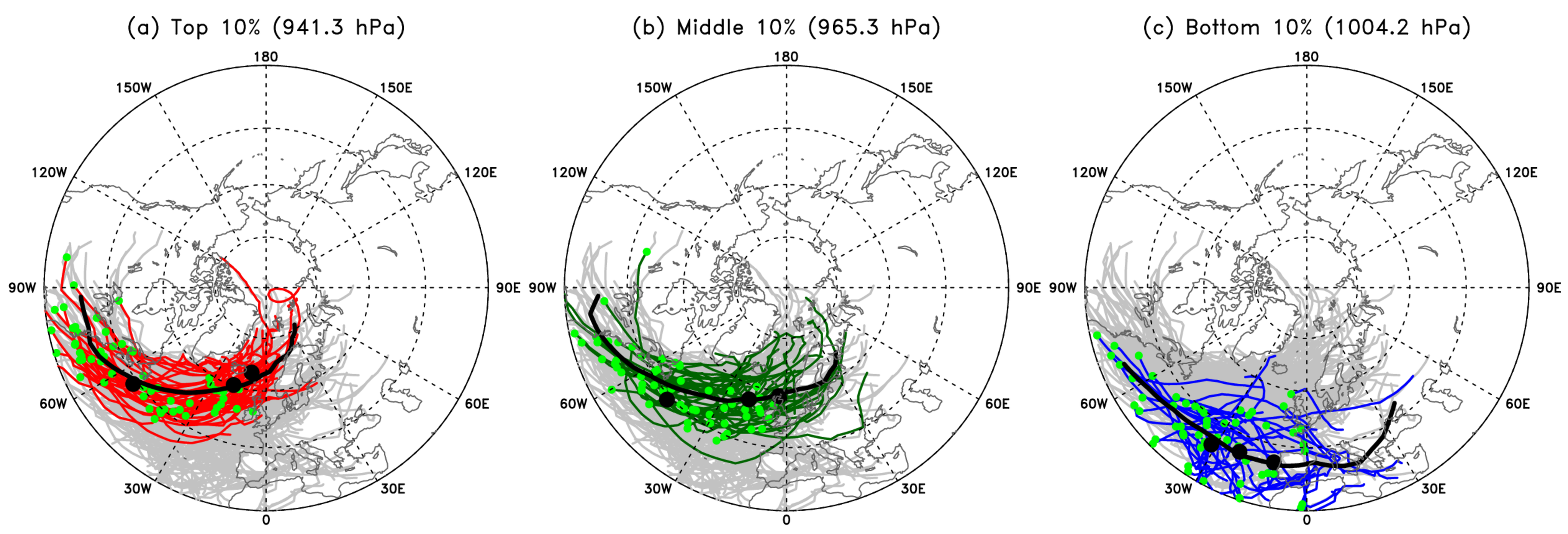

Figure 1. Atlantic windstorm tracks classified according to maximum intensity (minimum central pressure). The detected number of Atlantic windstorms in winter of 1981-2016 is 591 and each extreme storm case is 59. Gray, red, dark green, blue, and black lines, respectively, indicate tracks of total, strong (a), middle (b), weak (c) storms, and their mean paths. Light green dots represent each storm centers at cyclogenesis step. Black dots in a sequential order from left to right are mean locations of cyclogenesis, maximum intensity step, and cyclolysis, respectively. The numbers in parentheses on each figure are averaged minimum central pressures.

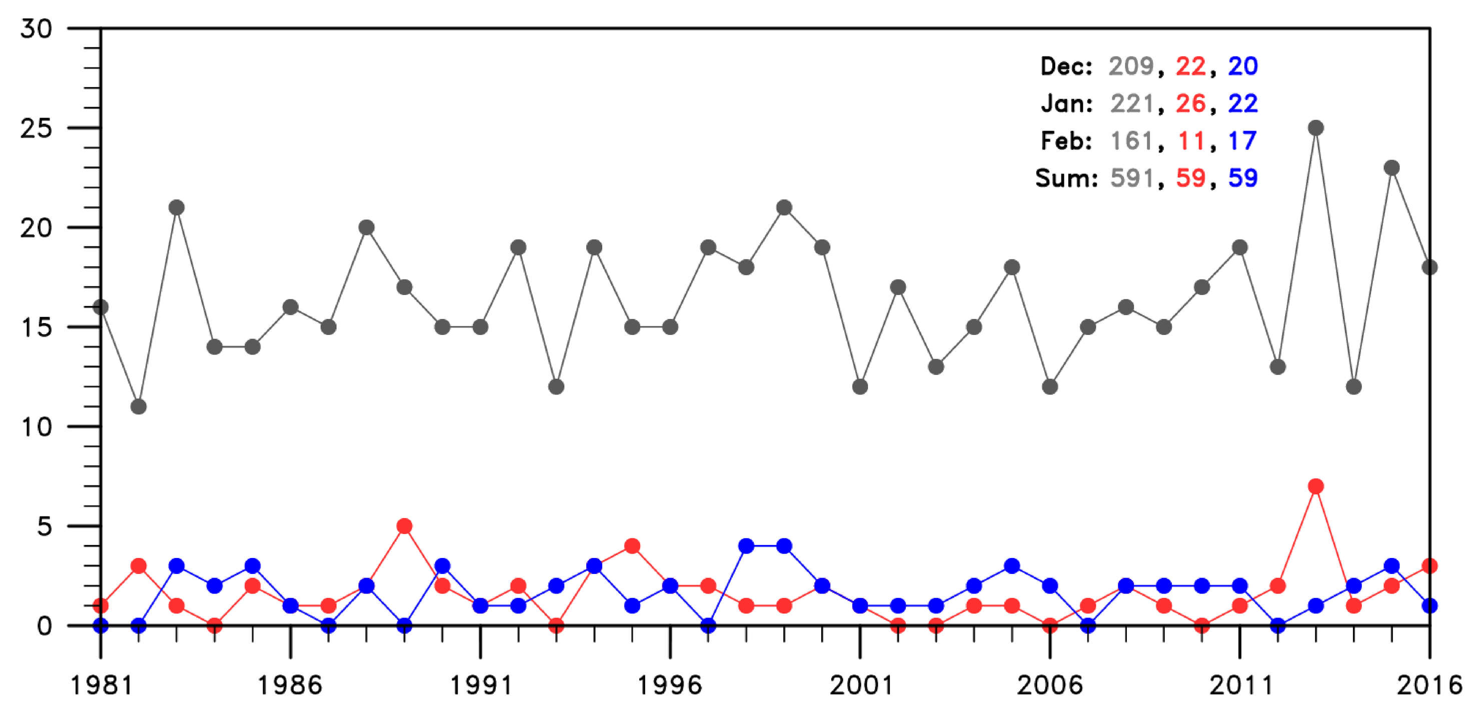

Supplementary figure 1. Time series of the total (gray), strong (red), and weak (blue) number of Atlantic windstorms for 36 winters. The numbers of storms are 591 for total, and 59 for both strong and weak windstorms. The numerals in the figure are the numbers of occurrences of total, strong, and weak storms in December, January, February, and their summation.

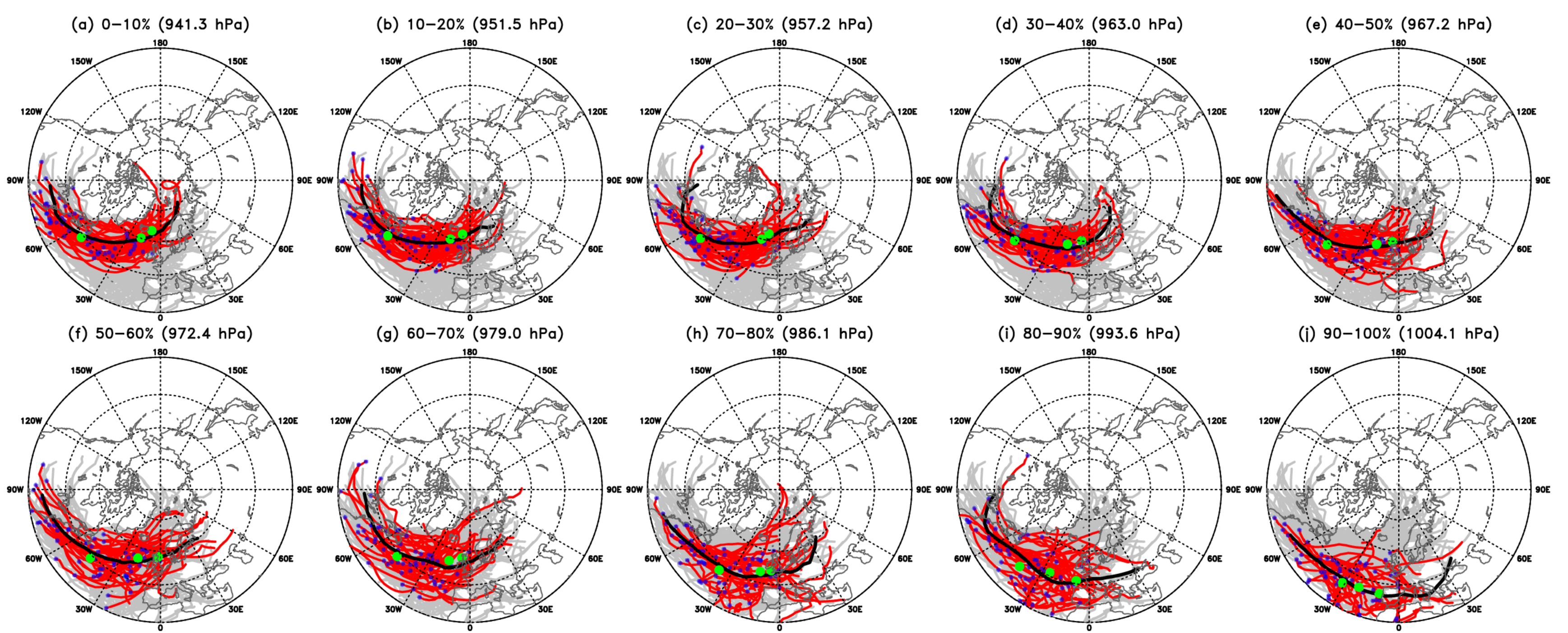

Supplementary figure 2. Atlantic windstorm tracks classified according to maximum intensity. Total number of Atlantic windstorms in winter is 591 and each case storm is 59 except for 90-100% (60). (a) is top 10% storms and (j) is bottom 10% storms. Gray, red, and black lines, respectively, indicate tracks of all storms, every 10% storms, and their mean paths. Blue dots represent each storm centers at cyclogenesis step. Green dots in a sequential order from left to right are mean locations of cyclogenesis, maximum intensity step, and cyclolysis, respectively. The numbers in parentheses on each figure are averaged minimum central pressures.

3. Composites

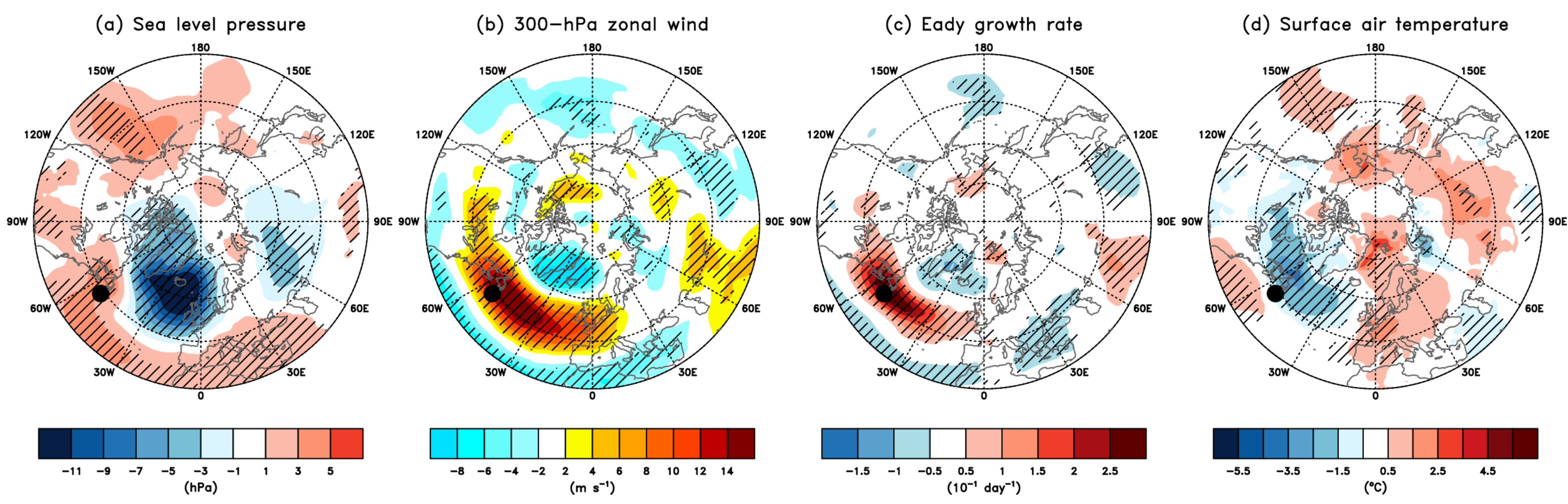

Figure 2. Initial state of strong storms. Daily composites of anomalous sea level pressure (**a**), 300-hPa zonal wind (**b**), Eady growth rate between 200 and 850 hPa (**c**), and surface air temperature (**d**) on the cyclogenesis date of top 10% storms. Black dots are mean locations of top 10% cyclogenesis. Only values exceeding 10% significance level area hatched.

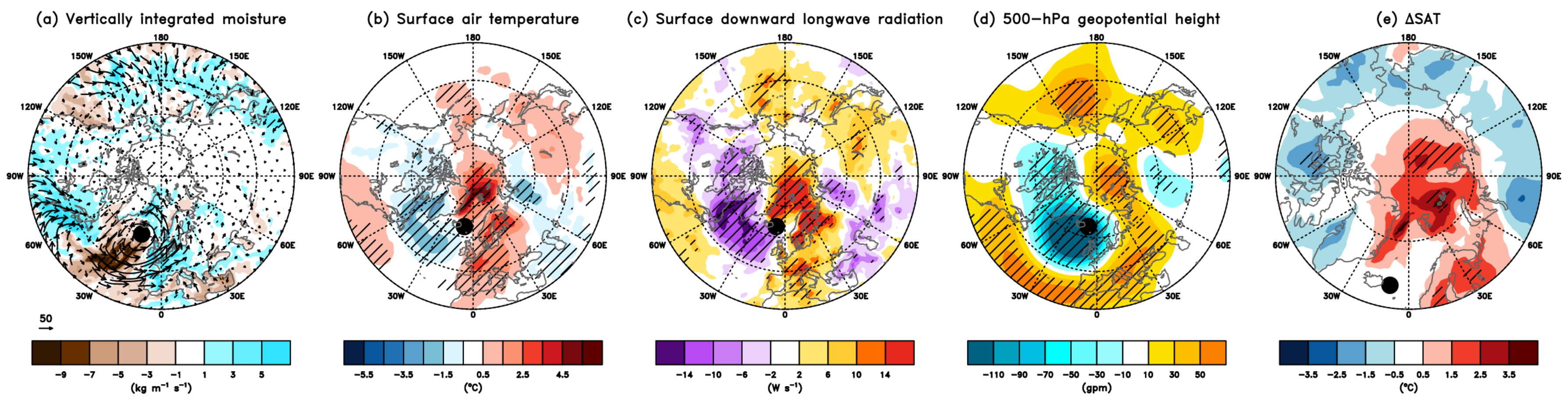

Figure 3. Peak and dissipation state of strong storms. Same as Fig. 2, but for vertically integrated horizontal moisture flux (arrows) and its convergence (shading) on peak dates of strong storms (**a**), surface air temperature (**b**), surface downward longwave radiation (**c**), 500-hPa geopotential height (**d**) on cyclolysis dates of strong storms, and temperature difference between cyclolysis and cyclogenesis dates (**e**). Black dots are average locations of each storm state.

Supplementary table 1. The change in surface air temperature over Barents-Kara Seas (75°-90°N, 0°-90°E) between cyclolysis and cyclogenesis dates (ΔSAT) at each storm intensity level. An asterisk denotes the statistical significance at the 1 % significance level.

Top (%)	10	10-20	20-30	30-40	40-50	50-60	60-70	70-80	80-90	90-100
Mean (°C)	2.02*	0.21	0.22	0.18	-0.53	-0.68	0.04	-0.70	-0.89	-0.42

4. Model simulations

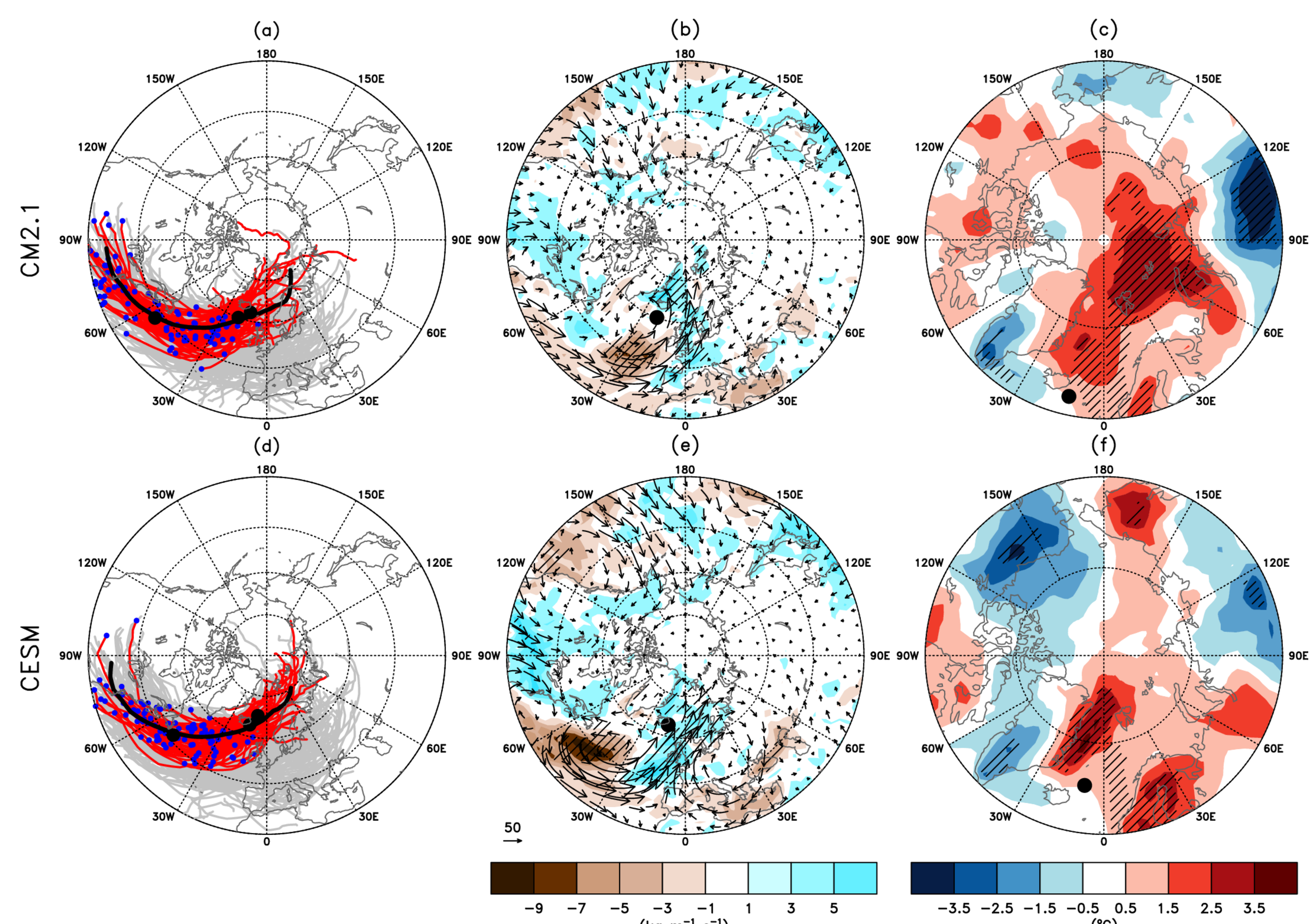

Figure 4. Simulated characteristics in top 10% Atlantic windstorms. a,d, The same as in Fig. 1a, but for CM2.1 (**a**) and CESM (**d**). The detected number of Atlantic windstorms for 100 winters of CM2.1 and CESM are 911 and 922, respectively. Averaged minimum central pressures of top 10% storms of CM2.1 and CESM are 944.4 hPa and 939.7 hPa, respectively. **b,e,** The same as in Fig. 3a, but for CM2.1 (**b**) and CESM (**e**). **c,f,** The same as in Fig. 3e, but for CM2.1 (**c**) and CESM (**f**).

5. Conclusion

- In summary, top 10% Atlantic windstorms tend to northeastward between Greenland and Svalbard while bottom 10% storms are inclined to go eastward towards Western Europe without change the number of storm occurrences in recent decades, and these are simulated in model results also. Composite analyses show that top 10% storms statistically develop under a positive NAO pattern, associated with enhanced jet stream and baroclinicity, and increased meridional temperature gradient over North Atlantic. These conditions help to foster growth of top 10% storms. In accordance with previous studies, we reveal that anomalous moisture transports into Arctic during storm lifetime is important for Arctic warming, particularly Barents-Kara Seas. After the breaking of top 10% storms, surface downward longwave radiation is observed to increase over the Atlantic sector of the Arctic and Barents-Kara Seas. The middle tropospheric geopotential height anomaly is positive over the Europe and near the Ural Mountains. That reflects the occurrence of blocking induced by strong storms. These mechanisms contribute to the warming over Arctic, especially Barents-Kara Seas. Model experiments simulate similar composite patterns to observation. This finding suggests the importance of poleward energy transport by moist air intrusion from mid-latitude to the Arctic as a contributing factor of the Arctic warming.

WCRP/SPARC Local Workshop | Korea Polar Research Institute, Incheon, Korea | October 19–20 2017